Eutectic Phenomenon of LiNH$_2$-KH Composite in MH-NH$_3$ Hydrogen Storage System

Kiyotaka Goshome [1] **, Ankur Jain** [2,*] **, Hiroki Miyaoka** [2] **, Hikaru Yamamoto** [2] **, Yoshitsugu Kojima** [2,3] **and Takayuki Ichikawa** [2,4,*]

[1] Renewable Energy Research Center, National Institute of Advanced Industrial Science and Technology, 2-2-9 Machiikedai, Koriyama, Fukushima 963-0298, Japan; goshoume.kiyotaka@aist.go.jp

[2] Natural Science Center for Basic Research and Development, Hiroshima University, 1-3-1 Kagamiyama, Higashi-Hiroshima 739-8530, Japan; miyaoka@h2.hiroshima-u.ac.jp (H.M.); mhikaru@h2.hiroshima-u.ac.jp (H.Y.); kojimay@hiroshima-u.ac.jp (Y.K.)

[3] Graduate School of Advanced Sciences of Matter, Hiroshima University, 1-3-1 Kagamiyama, Higashi-Hiroshima 739-8530, Japan

[4] Graduate School of Engineering, Hiroshima University, 1-4-1 Kagamiyama, Higashi-Hiroshima 739-8527, Japan

* Correspondence: ankur.j.ankur@gmail.com (A.J.); tichi@hiroshima-u.ac.jp (T.I.)

check for updates

Abstract: Hydrogenation of a lithium-potassium (double-cation) amide (LiK(NH$_2$)$_2$), which is generated as a product by ammonolysis of litium hydride and potassium hydride (LiH-KH) composite, is investigated in details. As a result, lithium amide (LiNH$_2$) and KH are generated after hydrogenation at 160 °C as an intermediate. It is noteworthy that the mixture of LiH and KNH$_2$ has a much lower melting point than that of the individual melting points of LiNH$_2$ and KH, which is recognized as a eutectic phenomenon. The hydrogenation temperature of LiNH$_2$ in the mixture is found to be significantly lower than that of LiNH$_2$ itself. This improvement of reactivity must be due to kinetic modification, induced by the enhanced atomic mobility due to the eutectic interaction.

**Keywords:** hydrogen carrier; ammonia; metal hydride; double-cation amide; eutectic melting

1. Introduction

The use of hydrogen energy has attracted attention for the introduction of renewable energy [1]. Since renewable energy fluctuates significantly depending on the season, weather, and location, it is necessary to stably store and transport it by conversion to a suitable chemical energy. Hydrogen can be produced by water electrolysis using renewable energy-based power sources, and stored compactly at low pressure by using a hydrogen storage alloy [2]. Finally, hydrogen can be used with a fuel cell to obtain electric and heat power according to demand [3]. In terms of hydrogen transportation, gravimetric hydrogen density of hydrogen storage alloys are generally lower than 2 wt%, which is insufficient for transportation application [4]. Compressed and liquid hydrogen are the options; however, there are some problems to be solved for practical use (e.g., development of a lightweight pressure-tight tank, a durable hydrogen compressor, a cryogenic insulation container, a cryogenic liquid pump, and so on) [5]. Hydrides composed of light elements (e.g., LiH, NaBH$_4$, CH$_4$, BH$_3$NH$_3$, NH$_3$, LiNH$_2$, MgH$_2$, and NaAlH$_4$) are expected to be promising hydrogen storage materials, which can store hydrogen with high gravimetric and volumetric hydrogen density at moderate conditions [5–8]. Numerous studies for hydrogen storage properties of the hydrides and their combinations have been reported so far. The combination of solid hydrides (i.e., LiH and LiNH$_2$) is one of the most notable systems and is known as an amide-imide (*M*-N-H) hydrogen storage system [9–15]. The first report of

the above system was published by Chen et al. in 2002 [16]. The hydrogen absorption and desorption reaction with the high hydrogen capacity of 6.5 mass% proceeds as follows,

$$LiH + LiNH_2 \leftrightarrow Li_2NH + H_2 \tag{1}$$
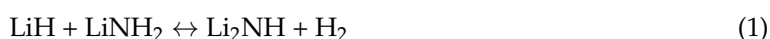
The enthalpy change of the hydrogen release (ΔH_{des}) by reaction (1) has been reported to be 65.6 kJ mol^{-1} H$_2$ [17]. The equilibrium temperature was estimated to be 234 °C to obtain 1 atm of equilibrium hydrogen pressure when the entropy change was assumed as 130 J mol^{-1} K^{-1} [18]. To modify the thermodynamics, other M-N-H systems with alternative metals (e.g., K, Na, Ca, and Mg) have been studied so far. Besides, many researchers have studied these systems to reveal the reaction mechanism. Ichikawa et al. have clarified that the de/re-hydrogenation reaction is composed of two-step reactions, including the decomposition of LiNH$_2$ to generate NH$_3$ as follows [19],

$$2LiNH_2 \leftrightarrow Li_2NH + NH_3 \tag{2}$$

$$LiH + NH_3 \leftrightarrow LiNH_2 + H_2 \tag{3}$$
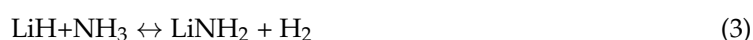
Improving the kinetics of the de/re-hydrogenation, and suppressing the emission of NH$_3$ gas by reaction (2), could be achieved by using various catalysts, such as KOH, TiCl$_3$, LiTi$_2$O$_4$, CeF$_4$, etc. [15].

The metal hydride-ammonia (MH-NH$_3$) hydrogen storage system was derived from the reaction in the equation (3). By using this system, H$_2$ can be desorbed and absorbed below 300 °C [20–24]. Here, NH$_3$ has a top-class hydrogen capacity; the gravimetric density is 17.8 mass%, and it condenses at 25 °C when pressurized to 1 MPa. Therefore, the MH-NH$_3$ system is also regarded as a high gravimetric and volumetric hydrogen carrier (M = Li; 8.1 wt%, 4.5 kg /100 L) [21]. Previously, it was experimentally revealed that the exothermic ammonolysis of MH to generate H$_2$ proceeds at room temperature [21,22,25–29]. Besides, the hydrogenation of MNH$_2$ to form MH and NH$_3$ can proceed below 300 °C. The reaction rate of both ammonolysis and hydrogenation become higher in the order of elements placed in the periodic table (K > Na > Li) [22]. Therefore, the kinetics of the LiH-NH$_3$ system with the highest gravimetric hydrogen density needs to be improved. In previous work, we investigated the LiH-KH composite NH$_3$ system [30]. The reaction rate of the ammonolysis of the LiH-KH composite was found to be improved by a synergetic effect. Here, a new double-cation metal amide phase (i.e., LiK(NH$_2$)$_2$) was reported to be formed as a reaction product. Interestingly, the complete hydrogenation of complex LiK(NH$_2$)$_2$ proceeded at a much lower temperature than that of LiNH$_2$. In this work, thermal and hydrogenation properties of complex LiK(NH$_2$)$_2$ are investigated in further detail to understand its reaction mechanism, which would be useful and applicable to some related M-N-H systems.

2. Results and Discussion

2.1. Investigation for Hydrogenation of Complex LiK(NH$_2$)$_2$ at Lower Temperature

The hydrogenation of amides (M(NH$_2$)$_m$) proceeds by the following reaction,

$$M(NH_2)_m + mH_2 \rightarrow MH_m + mNH_3 \tag{4}$$
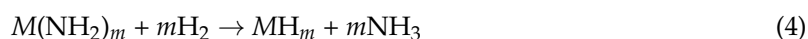
where m represents the stoichiometric coefficient and is equal to the valence number of the metal cation (M^{m+}). The hydrogenation reaction proceeds through an ion-exchange reaction between solid M(NH$_2$)$_m$ and gaseous H$_2$, that is, amide ions (NH$_2{}^-$) in M(NH$_2$)$_m$ are replaced by hydride ions (H$^-$) to form solid MH$_m$ and gaseous NH$_3$. Thus, the weight loss during the hydrogenation is shown due to the weight difference between M(NH$_2$)$_m$ and MH$_m$. The reaction yield (Y) is estimated by the weight loss of the solid samples after the hydrogenation by the following equation,

$$Y = 100 \cdot |\Delta w| \cdot W_{M(NH2)m} / (m \cdot w \cdot W_{NH}) \tag{5}$$

where w, Δw, $W_{M(NH2)_m}$, and W_{NH} represent the weight of the sample before the reaction, the weight loss of the sample due to the hydrogenation, the molecular weight of $M(NH_2)_m$, and NH, respectively. The hydrogenation of complex $LiK(NH_2)_2$ was performed under hydrogen flow condition at adequate flow rate as compared to a small amount of sample; therefore, the generated NH_3 was removed continuously from the reaction field to maintain the non-equilibrium condition during the reaction [31]. Thus, the endothermic hydrogenation could proceed even below 300 °C.

Figure 1a shows the thermal desorption mass spectroscopy (TD-MS) profile of complex $LiK(NH_2)_2$ under 0.5MPa H_2 flow condition during heating process to 160 °C and the isothermal step for 1 h. In the TD-MS profile, a peak corresponding to NH_3 was originated at 80 °C, which decreased during the isothermal step, suggesting that the hydrogenation by the reaction described in Equation (4) proceeded to form NH_3. The reaction yield was only 56.3%, which means that half the amount of metal amides remained unreacted.
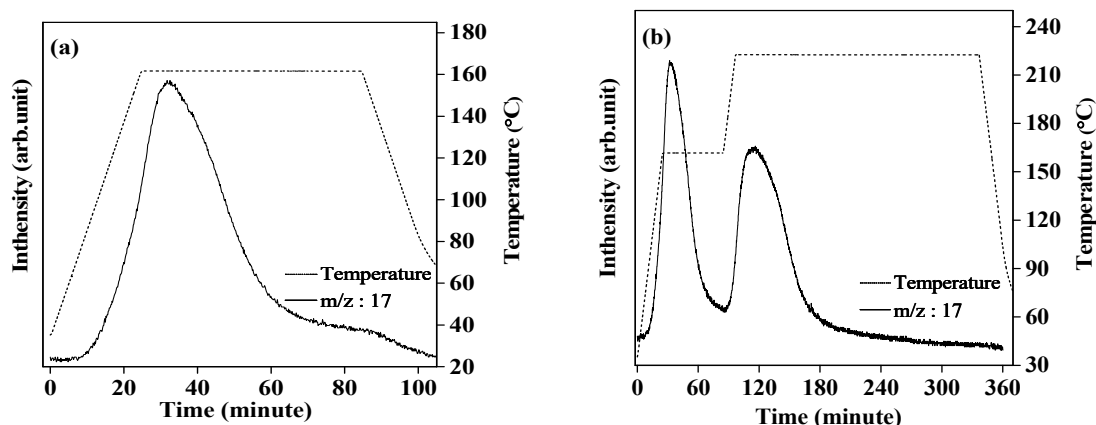

Figure 1. Thermal desorption mass spectroscopy (TD-MS) profile of complex $LiK(NH_2)_2$ under 0.5 MPa H_2 flow condition at 160 °C for 1 h (**a**), and following 220 °C for 4 h (**b**), where the heating rate is 5 °C/min and m/z is 17 for NH_3.

Figure 2a,b show X-ray diffraction (XRD) patterns of the samples before and after the hydrogenation at 160 °C for 1 h. The peaks of complex $LiK(NH_2)_2$ phase completely disappeared, and the diffraction patterns corresponded to the KH and $LiNH_2$ phases. It was considered that KH and $LiNH_2$ were formed by the reaction of complex $LiK(NH_2)_2$ with H_2 below 160 °C, in other words, the K–related components in the complex amide selectively reacted with H_2 prior to the reaction of the Li-related component. The phase variation at 160 °C was consistent with the above approximately 50% reaction yield, estimated from the weight change, because the atomic ratio of Li:K in the complex $LiK(NH_2)_2$ was 1. Here, the slightly excess reaction yield, beyond 50%, must be caused by the partial hydrogenation of the $LiNH_2$ component; however, the diffraction peaks corresponding to LiH could not be detected by XRD because of the small amount and low diffraction intensity, which was due to the low electron number. The above consideration about the reactivity of KNH_2 and $LiNH_2$ components was consistent with the previous reports. The complex $LiK(NH_2)_2$ was hydrogenated to form a mixture of $LiNH_2$ and KH through the formation of $LiK_3(NH_2)_4$ as an intermediate [30]. Besides, the hydrogenation of KNH_2 under H_2 flow condition proceeded even at 50 °C, which was significantly lower than that of $LiNH_2$ [22]. The above results indicate that the molecular properties of KNH_2 and $LiNH_2$ remained intact in $LiK(NH_2)_2$ and strongly affected the hydrogenation properties, even though crystal structure of the complex amide was different from those of the single cation amides.
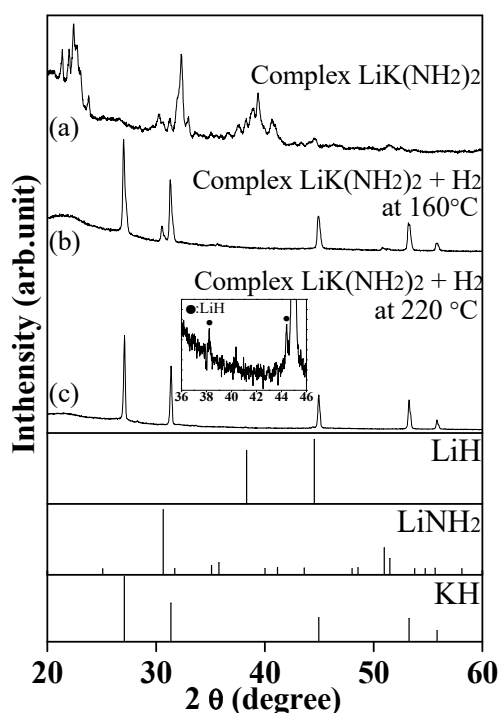
Figure 2. X-ray diffraction (XRD) patterns of complex LiK(NH$_2$)$_2$ before (**a**) and after (**b**) the hydrogenation at 160 °C for 1 h, and following 220 °C for 4 h (**c**). The inset shows the enlarged figure for profile (**c**) to find the peaks of LiH; XRD pattern of LiH (PDF#78-0838), LiNH$_2$ (PDF#75-0049), and KH (PDF#65-9244) are referred from databases.

In order to understand the thermal properties of the hydrogenated product of LiK(NH$_2$)$_2$ at 160 °C (i.e., the mixture of LiNH$_2$ and KH), the differential scanning calorimetery (DSC) measurement under 0.5 MPa H$_2$ atmosphere in a closed condition was performed, where the H$_2$ atmosphere prevents the H$_2$ desorption from the mixture of LiNH$_2$ and KH by the equivalent process, described as Equation (1). A reversible sharp peak around 240 °C was observed in the DSC profile (Figure S1). Since no phase transition is known for either LiNH$_2$ or KH at this temperature, this reversible peak suggested a possibility of melting; however, the melting point of both of LiNH$_2$ and KH are also higher than 350 °C [22,32]. Therefore, the phase transition must have originated in the coexistence of KH and LiNH$_2$, indicating a eutectic melting phenomenon. To further understand the reversible change of the mixture during the DSC measurement, and to confirm whether it is melting or not, the thermal behavior of a ball-milled mixture of KH and LiNH$_2$ (similar to the hydrogenation product of complex LiK(NH$_2$)$_2$) was investigated by the DSC measurements.

Figure 3 shows the DSC profile for the ball-milled mixture of KH and LiNH$_2$ in the temperature range from room temperature (RT, 22 °C) to 270 °C under 0.5 MPa H$_2$ atmosphere in the closed condition. The ball-milled mixture of KH and LiNH$_2$ showed a similar reversible sharp peak around 240 °C. It is noteworthy that the temperatures of these peaks were not shifted even under the different H$_2$ pressures (Figure S2), indicating that the reversible peaks were not originated due to de/re-hydrogenation. Besides, the sample after the DSC measurement was in a lump state, as shown in the insert image of Figure 3. Moreover, the XRD results of the sample before and after DSC measurement confirmed the existence of LiNH$_2$ and KH phases, as shown in Figure 4. Thus, it was experimentally revealed that a mixture of LiNH$_2$ and KH shows the eutectic phenomenon. Herein, the composition of the mixture of LiNH$_2$/KH is not necessarily in a eutectic composition and might show a suspension after the melting. The accurate eutectic composition will be revealed by performing DSC measurements for the mixture of various compositions in the future.
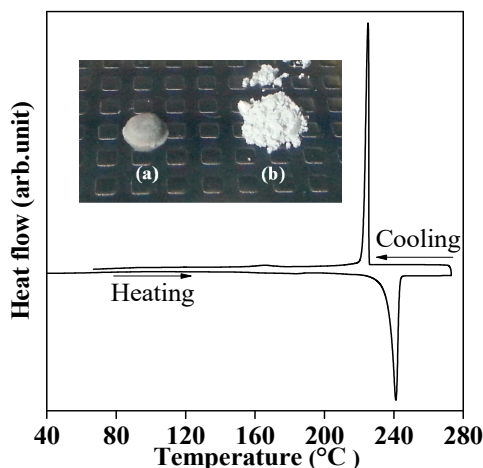
Figure 3. Differential scanning calorimetery (DSC) profile of the ball-milled mixture of $LiNH_2$ and KH. The DSC was performed under 0.5 MPa H_2 atmosphere in closed condition up to 270 °C, with heating rate of 5 °C/min. The inset shows the appearance of the ball-milled mixture of KH and $LiNH_2$ before (**b**) and after (**a**) the DSC measurement.
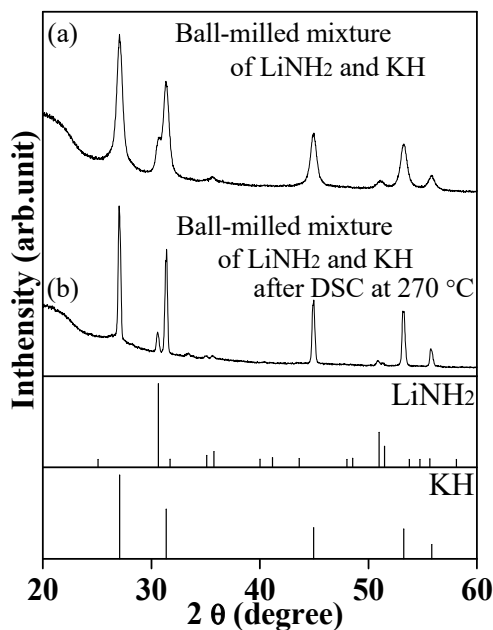

Figure 4. XRD patterns of the ball-milled mixture of $LiNH_2$ and KH before (**a**) and after (**b**) DSC measurement under H_2 atmosphere up to 270 °C with a heating rate of 5 °C/min; XRD patterns of $LiNH_2$ (PDF#75-0049) and KH (PDF#65-9244) are referred from databases.

2.2. Investigation for Hydrogenation of Complex $LiK(NH_2)_2$ at Higher Temperature

Further hydrogenation of the mixture of $LiNH_2$ and KH, produced from the partial hydrogenation at 160 °C, was performed at 220 °C, which is lower than that of the eutectic melting point to avoid the influence of the phase transition, such as the decrease in surface area by melting. Figure 1b shows TD-MS profile of complex $LiK(NH_2)_2$ under 0.5 MPa H_2 flow condition up to 220 °C; the temperature was increased and kept at 160 °C for 1 h and 220 °C for 4 h during the DSC scan. The intensity of the MS peak corresponding to NH_3 obviously increased above 180 °C after the first reaction at 160 °C, which should be attributed to the hydrogenation of the residual $LiNH_2$. In fact, XRD results in Figure 2c showed the diffraction pattern of KH without that of $LiNH_2$. The existence of LiH was also confirmed in the enlarged XRD profile between 36 to 46 of 2θ range. The total reaction yield was found to be 95.6% and indicated the complete hydrogenation of complex $LiK(NH_2)_2$. In this view,

the reaction yield in this work was much higher than the previous reports. Yamamoto et al. reported that the reaction yield for hydrogenation of single $LiNH_2$ was 4.2% at 200 °C for 4 h and 71.0% at 300 °C [22]. Dong et al. reported that the reaction yield for hydrogenation of single $LiNH_2$ was 24.3% at 200 °C for 4 h [24]. Even though it is difficult to directly compare our results with these previous reports because of the difference in H_2 flow rate, reaction scale, and any other reaction conditions, it can be concluded that the hydrogenation performance of complex $LiK(NH_2)_2$ was obviously improved as compared with the $LiNH_2$ itself, because it showed almost 100% hydrogenation at a relatively lower temperature and shorter retention time for the reaction. Furthermore, it can be suggested that the high reactivity of $LiNH_2$ in the mixture at 220 °C originated from the eutectic interaction between KH and $LiNH_2$. As a similar phenomenon, Yamamoto et al. [22] reported a sudden change in the hydrogenation of $NaNH_2$ at around 200 °C; the temperature was quite close to the melting point of $NaNH_2$ at 210 °C [33]. As described above, the melting point of $LiNH_2$ was lowered down to about 240 °C by the eutectic interaction with KH. Particularly, the atoms in the solid phase possibly became active with high mobility near the melting point, resulting in high reactivity with H_2 to form NH_3. Such atomic mobility is important for the hydrogenation of complex $LiK(NH_2)_2$, because it is necessary to release heavy N atoms in the form of NH_3.

A lot of studies for *M*-N-H systems with various combinations of $M_I(NH_2)_m$-$M_{II}H_n$ composites (M_I, M_{II} = Li, Na, K, Ca, Mg with the valence number of M_I and M_{II} cations as *m* and *n*) have been published before [34–42]. To cite an instance, an interaction between $Mg(NH_2)_2$ and LiH, known as Li-Mg-N-H system, has been regarded as one of the most practicable hydrogen storage material, because it can generate 5.5 mass% of H_2 and be re-hydrogenated under 150 °C by the following reaction [43–45],

$$Mg(NH_2)_2 + 2LiH \leftrightarrow MgLi_2(NH)_2 + 2H_2 \tag{6}$$
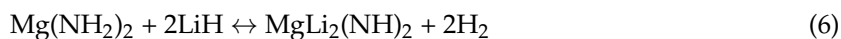
Although the Li-Mg-N-H system has suitable thermodynamics (i.e., ΔH_{des} of -38.9 kJ mol^{-1} H_2) and is expected to show desorption pressure of 0.1 MPa at <90 °C, its slow reaction rate is still the main issue for its practical use [46]. Thus, many approaches to improve the de/re-hydrogenation kinetics of the Li-Mg-N-H system have been reported [47–51]. It is noted that the eutectic melting phenomenon of $M_I(NH_2)_m$-$M_{II}H_n$ would be important as an advantage for such *M*-N-H system. As described above, the de-hydrogenation of the *M*-N-H system proceeds in the solid–solid reaction; therefore, the contact between the particles should be an important factor. Besides, it is reported that the de-hydrogenation process includes a decomposition process of metal amide to generate NH_3 as an intermediate, then the decomposition could directly affect the de-hydrogenation rate. In this view, Leng et al. reported the decomposition properties of several metal amides [35]. Using the thermogravimetry-differential thermal analysis (TG-DTA), they have shown the two-step decomposition of $LiNH_2$ at different temperatures. They claimed that these steps are originated in the decomposition on the surface at a lower temperature and in the bulk at higher temperature. Interestingly, the decomposition of the second step is likely to occur near the melting point of $LiNH_2$ and due to the modification of the atomic mobility in the solid by the melting. From the above considerations of the contact between the particles and the decomposition rate of metal amide in the de-hydrogenation process of the *M*-N-H system, the melting phenomenon of the $M_I(NH_2)_m$-$M_{II}H_n$ composite should have a significant effect on the reaction kinetics. However, the melting phenomenon of the $M_I(NH_2)_m$-$M_{II}H_n$ composite has not been studied so far. In this work, the eutectic melting phenomenon of the mixture of KH and $LiNH_2$ has been revealed for the first time by performing the thermal investigation in an unusual circumstance, that is a compressed H_2 environment. Recently, Dong et al. reported that dehydrogenation properties of the Li-N-H system was improved by doping 1–10 mol% KH [52]; the eutectic phenomenon could be believed to be one of the factors for the improvement. Thus, a systematic detailed investigation of such eutectic melting phenomena is expected to lead to a breakthrough for the development of a novel *M*-N-H system in future.

3. Materials and Methods

Lithium hydride (LiH) (99.4%, Alfa aesar), potassium hydride (KH) (dispersion in mineral oil, Aldrich), lithium amide ($LiNH_2$) (95%, Aldrich), and potassium amide (KNH_2), synthesized by the reaction of KH with NH_3 (99.999%), were used for the experiments. The KH with mineral oil was introduced into anhydrous tetrahydrofuran (THF) (>99.9%, Aldrich) and stirred for 3 min. Then, the supernatant solution was drained to remove the mineral oil. The above procedure was repeated 5 times. Finally, the slurry of the KH was evacuated for 5 h to completely remove the remaining THF. The complex $LiK(NH_2)_2$ was prepared by the milling of LiH and KH with a 1:1 molar ratio in a stainless steel container with twenty 7-mm steel balls, at 370 rpm for 10 h under 1.0 MPa H_2 atmosphere, by using a planetary ball mill apparatus (Fritsch, P7). Then, this milled LiH-KH composite was heat-treated at 220 °C under 1.0 MPa H_2 atmosphere and reacted with 0.8 MPa NH_3 at room temperature to form complex $LiK(NH_2)_2$ [30]. A ball-milled mixture of $LiNH_2$ and KH, with a molar ratio of LiNH2/KH = 1, was prepared by ball-milling for 10 h under 0.1 MPa Ar atmosphere. The samples were examined by X-ray diffraction (XRD) (Rigaku, RINT-2100) using Cu Kα radiation. The samples were sensitive to air and handled in a glove box (Miwa MFG, MP-P60 W) filled with highly pure Ar (>99.9999%).

Investigation for hydrogenation of complex $LiK(NH_2)_2$ was performed by thermal desorption mass spectroscopy (TD-MS) (Canon Anelva Corporation, M-100QA) (Kawasaki, Japan) under 0.5 MPa H_2 flow condition at 200 sccm (= cc/min at 0.1 MPa, 0 °C), where 5 mg and/or less amount of sample was used. The weight of the sample before and after the TD-MS measurement was measured to estimate the reaction yield. The products, after the TD-MS measurements, were identified by XRD measurement.

Thermal properties of the mixture of $LiNH_2$ and KH were investigated under 0.5–2 MPa H_2 atmosphere by differential scanning calorimetry (DSC) (TA Instruments, Q10 PDSC). The products after the DSC measurements were identified by XRD measurement.

4. Conclusions

The hydrogenation reaction of complex $LiK(NH_2)_2$ is found to occur at 220 °C under H_2 flow condition completely, which is lower than that of $LiNH_2$. The hydrogenation was proceeded by two step reactions. At the first step, the hydrogenation of the KNH_2 component in the complex amide occurred to form KH and NH_3 below 160 °C, followed by the hydrogenation of $LiNH_2$ to form LiH and NH_3 at 220 °C. In this case, the reactivity of $LiNH_2$ could be enhanced by the eutectic interaction with KH. Thus, it has been clarified that not only ammonolysis but also the hydrogenation of the LiH-NH_3 system can be improved by the interaction with KH. In the future, the eutectic melting phenomena of the $M_I(NH_2)_m$-$M_{II}H_n$ composite will be investigated in further detail.

References

1. Hanley, E.S.; Deane, J.P.; Gallachoir, B.P.O. The role of hydrogen in low carbon energy futures—A review of existing perspectives. *Renew. Sustain. Energy Rev.* **2018**, *82*, 3027–3045. [CrossRef]
2. Endo, N.; Suzuki, S.; Goshome, K.; Maeda, T. Operation of a bench-scale TiFe-based alloy tank under mild conditions for low-cost stationary hydrogen storage. *Int. J. Hydrogen Energy* **2017**, *42*, 5246–5251. [CrossRef]
3. Veras, T.D.; Mozer, T.S.; dos Santos, D.; Cesar, A.D. Hydrogen: Trends, production and characterization of the main process worldwide. *Int. J. Hydrogen Energy* **2017**, *42*, 2018–2033. [CrossRef]
4. Lototskyy, M.V.; Yartys, V.A.; Pollet, B.G.; Bowman, R.C. Metal hydride hydrogen compressors: A review. *Int. J. Hydrogen Energy* **2014**, *39*, 5818–5851. [CrossRef]
5. Zhang, F.; Zhao, P.C.; Niu, M.; Maddy, J. The survey of key technologies in hydrogen energy storage. *Int. J. Hydrogen Energy* **2016**, *41*, 14535–14552. [CrossRef]
6. Sinigaglia, T.; Lewiski, F.; Martins, M.E.S.; Siluk, J.C.M. Production, storage, fuel stations of hydrogen and its utilization in automotive applications—A review. *Int. J. Hydrogen Energy* **2017**, *42*, 24597–24611. [CrossRef]
7. Schlapbach, L.; Zuttel, A. Hydrogen-storage materials for mobile applications. *Nature* **2001**, *414*, 353–358. [CrossRef] [PubMed]
8. Lai, Q.W.; Paskevicius, M.; Sheppard, D.A.; Buckley, C.E.; Thornton, A.W.; Hill, M.R.; Gu, Q.F.; Mao, J.F.; Huang, Z.G.; Liu, H.K.; et al. Hydrogen Storage Materials for Mobile and Stationary Applications: Current State of the Art. *ChemSusChem* **2015**, *8*, 2789–2825. [CrossRef]
9. Hino, S.; Ichikawa, T.; Ogita, N.; Udagawa, M.; Fujii, H. Quantitative estimation of NH_3 partial pressure in H_2 desorbed from the Li-N-H system by Raman spectroscopy. *Chem. Commun.* **2005**. [CrossRef]
10. Ichikawa, T.; Hanada, N.; Isobe, S.; Leng, H.Y.; Fujii, H. Hydrogen storage properties in Ti catalyzed Li-N-H system. *J. Alloys Compd.* **2005**, *404*, 435–438. [CrossRef]
11. Isobe, S.; Ichikawa, T.; Hino, S.; Fujii, H. Hydrogen desorption mechanism in a Li-N-H system by means of the isotopic exchange technique. *J. Phys. Chem. B* **2005**, *109*, 14855–14858. [CrossRef] [PubMed]
12. Ichikawa, T.; Leng, H.Y.; Isobe, S.; Hanada, N.; Fujii, H. Recent development on hydrogen storage properties in metal-N-H systems. *J. Power Sources* **2006**, *159*, 126–131. [CrossRef]
13. Cao, H.J.; Wang, J.H.; Chua, Y.S.; Wang, H.; Wu, G.T.; Xiong, Z.T.; Qiu, J.S.; Chen, P. NH_3 Mediated or Ion Migration Reaction: The Case Study on Halide-Amide System. *J. Phys. Chem. C* **2014**, *118*, 2344–2349. [CrossRef]
14. Amica, G.; Larochette, P.A.; Gennari, F.C. Hydrogen storage properties of $LiNH_2$-LiH system with MgH_2, CaH_2 and TiH_2 added. *Int. J. Hydrogen Energy* **2015**, *40*, 9335–9346. [CrossRef]
15. Lin, H.J.; Li, H.W.; Murakami, H.; Akiba, E. Remarkably improved hydrogen storage properties of $LiNH_2$-LiH composite via the addition of CeF_4. *J. Alloys Compd.* **2018**, *735*, 1017–1022. [CrossRef]
16. Chen, P.; Xiong, Z.T.; Luo, J.Z.; Lin, J.Y.; Tan, K.L. Interaction of hydrogen with metal nitrides and imides. *Nature* **2002**, *420*, 302–304. [CrossRef] [PubMed]
17. Kojima, Y.; Kawai, Y. IR characterizations of lithium imide and amide. *J. Alloys Compd.* **2005**, *395*, 236–239. [CrossRef]
18. Osborn, W.; Markmaitree, T.; Shaw, L.L.; Hu, J.Z.; Kwak, J.; Yang, Z.G. Low temperature milling of the $LiNH_2$ + LiH hydrogen storage system. *Int. J. Hydrogen Energy* **2009**, *34*, 4331–4339. [CrossRef]
19. Ichikawa, T.; Hanada, N.; Isobe, S.; Leng, H.Y.; Fujii, H. Mechanism of novel reaction from $LiNH_2$ and LiH to Li_2NH and H_2 as a promising hydrogen storage system. *J. Phys. Chem. B* **2004**, *108*, 7887–7892. [CrossRef]
20. Leng, H.Y.; Ichikawa, T.; Hino, S.; Fujii, H. Investigation of reaction between $LiNH_2$ and H_2. *J. Alloys Compd.* **2008**, *463*, 462–465. [CrossRef]
21. Kojima, Y.; Tange, K.; Hino, S.; Isobe, S.; Tsubota, M.; Nakamura, K.; Nakatake, M.; Miyaoka, H.; Yamamoto, H.; Ichikawa, T. Molecular hydrogen carrier with activated nanohydride and ammonia. *J. Mater. Res.* **2009**, *24*, 2185–2190. [CrossRef]
22. Yamamoto, H.; Miyaoka, H.; Hino, S.; Nakanishi, H.; Ichikawa, T.; Kojima, Y. Recyclable hydrogen storage system composed of ammonia and alkali metal hydride. *Int. J. Hydrogen Energy* **2009**, *34*, 9760–9764. [CrossRef]
23. Dong, B.X.; Song, L.; Ge, J.; Teng, Y.L.; Zhang, S.Y. The ternary amide $KLi_3(NH_2)_4$: An important intermediate in the potassium compound-added Li-N-H systems. *RSC Adv.* **2014**, *4*, 10702–10707. [CrossRef]

24. Dong, B.X.; Teng, Y.L.; Ge, J.; Song, L.; Zhang, S.Y. The interesting and superior hydrogenation properties of potassium-doped LiNH$_2$ and its ternary mixed-cationic amide. *RSC Adv.* **2013**, *3*, 16977–16980. [CrossRef]

25. Hu, Y.H.; Ruckenstein, E. Ultrafast reaction between LiH and NH$_3$ during H$_2$ storage in Li$_3$N. *J. Phys. Chem. A* **2003**, *107*, 9737–9739. [CrossRef]

26. Miyaoka, H.; Fujii, H.; Yamamoto, H.; Hino, S.; Nakanishi, H.; Ichikawa, T.; Kojima, Y. Improvement of reaction kinetics by metal chloride on ammonia and lithium hydride system. *Int. J. Hydrogen Energy* **2012**, *37*, 16025–16030. [CrossRef]

27. Miyaoka, H.; Ichikawa, T.; Hino, S.; Kojima, Y. Compressed hydrogen production via reaction between liquid ammonia and alkali metal hydride. *Int. J. Hydrogen Energy* **2011**, *36*, 8217–8220. [CrossRef]

28. Teng, Y.L.; Ichikawa, T.; Miyaoka, H.; Kojima, Y. Improvement of hydrogen desorption kinetics in the LiH-NH$_3$ system by addition of KH. *Chem. Commun.* **2011**, *47*, 12227–12229. [CrossRef]

29. Miyaoka, H.; Nakajima, K.; Yamaguchi, S.; Aoki, T.; Yamamoto, H.; Okuda, T.; Goshome, K.; Ichikawa, T.; Kojima, Y. Catalysis of Lithium Chloride and Alkali Metal Borohydrides on Hydrogen Generation of Ammonia and Lithium Hydride System. *J. Phys. Chem. C* **2015**, *119*, 19922–19927. [CrossRef]

30. Goshome, K.; Miyaoka, H.; Yamamoto, H.; Ichikawa, T.; Kojima, Y. Hydrogen Ab/Desorption of LiH-KH Composite and Ammonia System. *Mater. Trans.* **2016**, *57*, 1215–1219. [CrossRef]

31. Goshome, K.; Miyaoka, H.; Ichikawa, T.; Yamamoto, H.; Ichikawa, T.; Kojima, Y. Ammonia Synthesis via Non-Equilibrium Reaction of Lithium Nitride in Hydrogen Flow Condition. *Mater. Trans.* **2015**, *56*, 410–414. [CrossRef]

32. Izuhara, T.; Takeshita, H.; Miyake, H. Thermodynamic Property Change in Li-N-H Hydrogen Storage System by Melting Lithium Amide. *J. Jpn. Inst. Met.* **2011**, *75*, 115–121. [CrossRef]

33. Wu, C.; Bai, Y.; Yang, J.H.; Wu, F.; Long, F. Characterizations of composite NaNH$_2$-NaBH$_4$ hydrogen storage materials synthesized via ball milling. *Int. J. Hydrogen Energy* **2012**, *37*, 889–893. [CrossRef]

34. Hu, J.; Xiong, Z.; Wu, G.; Chen, P.; Murata, K.; Sakata, K. Hydrogen releasing reaction between Mg(NH$_2$)$_2$ and CaH$_2$. *J. Power Sources* **2006**, *159*, 116–119. [CrossRef]

35. Leng, H.Y.; Ichikawa, T.; Hino, S.; Hanada, N.; Isobe, S.; Fujii, H. Synthesis and decomposition reactions of metal amides in metal-N-H hydrogen storage system. *J. Power Sources* **2006**, *156*, 166–170. [CrossRef]

36. Wu, G.; Xiong, Z.; Liu, T.; Liu, Y.; Hu, J.; Chen, P.; Feng, Y.; Wee, A.T.S. Synthesis and characterization of a new ternary imide-Li$_2$Ca(NH)$_2$. *Inorg. Chem.* **2007**, *46*, 517–521. [CrossRef]

37. Tokoyoda, K.; Hino, S.; Ichikawa, T.; Okamoto, K.; Fujii, H. Hydrogen desorption/absorption properties of Li-Ca-N-H system. *J. Alloys Compd.* **2007**, *439*, 337–341. [CrossRef]

38. Xiong, Z.; Wu, G.; Hu, J.; Chen, P. Ca-Na-N-H system for reversible hydrogen storage. *J. Alloys Compd.* **2007**, *441*, 152–156. [CrossRef]

39. Sheppard, D.A.; Paskevicius, M.; Buckley, C.E. Hydrogen Desorption from the NaNH$_2$-MgH$_2$ System. *J. Phys. Chem. C* **2011**, *115*, 8407–8413. [CrossRef]

40. Wang, J.H.; Wu, G.T.; Chua, Y.S.; Guo, J.P.; Xiong, Z.T.; Zhang, Y.; Gao, M.X.; Pan, H.G.; Chen, P. Hydrogen Sorption from the Mg(NH$_2$)$_2$-KH System and Synthesis of an Amide-Imide Complex of KMg(NH)(NH2). *Chemsuschem* **2011**, *4*, 1622–1628. [CrossRef]

41. Jain, A.; Miyaoka, H.; Ichikawa, T. Two-Peak Mystery of LiNH$_2$ NaH Dehydrogenation Is Solved? A Study of the Analogous Sodium Amide/Lithium Hydride System. *J. Phys. Chem. C* **2016**, *120*, 27903–27909. [CrossRef]

42. Nakamori, Y.; Kitahara, G.; Orimo, S. Synthesis and dehydriding studies of Mg-N-H systems. *J. Power Sources* **2004**, *138*, 309–312. [CrossRef]

43. Aoki, M.; Noritake, T.; Kitahara, G.; Nakamori, Y.; Towata, S.; Orimo, S. Dehydriding reaction of Mg(NH$_2$)$_2$-LiH system under hydrogen pressure. *J. Alloys Compd.* **2007**, *428*, 307–311. [CrossRef]

44. Leng, H.; Ichikawa, T.; Fujii, H. Hydrogen storage properties of Li-Mg-N-H systems with different ratios of LiH/Mg(NH$_2$)$_2$. *J. Phys. Chem. B* **2006**, *110*, 12964–12968. [CrossRef]

45. Leng, H.Y.; Ichikawa, T.; Hino, S.; Hanada, N.; Isobe, S.; Fujii, H. New metal-N-H system composed of Mg(NH$_2$)$_2$ and LiH for hydrogen storage. *J. Phys. Chem. B* **2004**, *108*, 8763–8765. [CrossRef]

46. Xiong, Z.T.; Hu, J.J.; Wu, G.T.; Chen, P.; Luo, W.F.; Gross, K.; Wang, J. Thermodynamic and kinetic investigations of the hydrogen storage in the Li-Mg-N-H system. *J. Alloys Compd.* **2005**, *398*, 235–239. [CrossRef]

47. Hu, J.J.; Liu, Y.F.; Wu, G.T.; Xiong, Z.T.; Chua, Y.S.; Chen, P. Improvement of hydrogen storage properties of the Li-Mg-N-H system by addition of LiBH$_4$. *Chem. Mater.* **2008**, *20*, 4398–4402. [CrossRef]

48. Wang, J.H.; Liu, T.; Wu, G.T.; Li, W.; Liu, Y.F.; Araujo, C.M.; Scheicher, R.H.; Blomqvist, A.; Ahuja, R.; Xiong, Z.T.; et al. Potassium-Modified $Mg(NH_2)_2/2$ LiH System for Hydrogen Storage. *Angew. Chem.-Int. Ed.* **2009**, *48*, 5828–5832. [CrossRef] [PubMed]

49. Pan, H.G.; Shi, S.B.; Liu, Y.F.; Li, B.; Yang, Y.J.; Gao, M.X. Improved hydrogen storage kinetics of the Li-Mg-N-H system by addition of $Mg(BH_4)_2$. *Dalton Trans.* **2013**, *42*, 3802–3811. [CrossRef]

50. Liang, C.; Liu, Y.F.; Gao, M.X.; Pan, H.G. Understanding the role of K in the significantly improved hydrogen storage properties of a KOH-doped Li-Mg-N-H system. *J. Mat. Chem. A* **2013**, *1*, 5031–5036. [CrossRef]

51. Miyaoka, H.; Wang, Y.M.; Hino, S.; Isobe, S.; Tokoyoda, K.; Ichikawa, T.; Kojima, Y. Kinetic Modification on Hydrogen Desorption of Lithium Hydride and Magnesium Amide System. *Materials* **2015**, *8*, 3896–3909. [CrossRef] [PubMed]

52. Dong, B.X.; Wang, L.; Ge, J.; Ping, C.; Teng, Y.L.; Li, Z.W. The effect of KH on enhancing the dehydrogenation properties of the Li-N-H system and its catalytic mechanism. *Phys. Chem. Chem. Phys.* **2018**, *20*, 11116–11122. [CrossRef] [PubMed]

Sample Availability: All the samples of the compounds are available from the authors.